Allosteric communication in the gating mechanism for controlled protein degradation by the bacterial ClpP peptidase

Special Collection: New Views of Allostery

Ashan Dayananda ⁽¹⁾; T. S. Hayden Dennison; Hewafonsekage Yasan Y. Fonseka ⁽¹⁾; Mohammad S. Avestan ⁽¹⁾; Qi Wang; Riina Tehver ⁽¹⁾; George Stan ⁽¹⁾



J. Chem. Phys. 158, 125101 (2023) https://doi.org/10.1063/5.0139184

CrossMark

View Online Export Citation

Articles You May Be Interested In

Genomic and proteomic analysis of Bacillus subtilis as microplastic bioremediation agents

AIP Conference Proceedings (January 2023)

Molecular analysis of Brevibacillus brevis as polyethylene biodegradation agents

AIP Conference Proceedings (January 2023)

Purification and proteolytic activity of Caseinolytic protease (Clp) from Lactobacillus plantarum IIA-1AS

AIP Conference Proceedings (November 2020)







Cite as: J. Chem. Phys. 158, 125101 (2023); doi: 10.1063/5.0139184

Submitted: 18 December 2022 • Accepted: 7 March 2023 •

Published Online: 27 March 2023







Ashan Dayananda, 1 📵 T. S. Hayden Dennison, 1 Hewafonsekage Yasan Y. 🛮 Fonseka, 🗀 📵 Mohammad S. Avestan, ¹ D Qi Wang, ^{1,b)} Riina Tehver, ^{2,c)} D and George Stan ^{1,c)} D

AFFILIATIONS

- ¹Department of Chemistry, University of Cincinnati, Cincinnati, Ohio 45221, USA
- ²Department of Physics and Astronomy, Denison University, Granville, Ohio 43023, USA

Note: This paper is part of the JCP Special Topic on New Views of Allostery.

- ^{a)}Present address: Biostatistics, Medpace, Inc., 5375 Medpace Way, Cincinnati, OH 45227, United States.
- b)Present address: Galixir Technologies, Beijing, China.
- c) Authors to whom correspondence should be addressed: tehverr@denison.edu and george.stan@uc.edu

ABSTRACT

Proteolysis is essential for the control of metabolic pathways and the cell cycle. Bacterial caseinolytic proteases (Clp) use peptidessenents, such as ClpPto degrade defective substrate proteins and to regulate cellular levels of stress-responseepsonesis salective degradationaccess to the proteolytic chamber of the double-ring ClpP tetradecamer is controlled by attinitionate chanism of the two axial pore-the binding of conserved loops of the Clp ATPase component of the protease or small synthesize or small synthesize. two axial pores he binding of conserved loops of the Clp ATPase component of the protease or small multipastes, yldepsipeptide (ADEP), at peripheral ClpP ring sitesiggers axial pore opening through dramatic conformational transitions of flexible N-termin loops between disordered conformations in the "closed" pore state and ordered hairpins in the "open" this estual type probe the allosteric communication underlying these conformational changes by comparing residue-residue couplings in molecular dynamics ulations of each configuration principal component and normal mode analyses highlight large-scale conformational changes in t N-terminal loop regions and smaller amplitude motions of the peptidase core. Community network analysis reveals a switch between and inter-protomer coupling in the open-closed pore translitiosteric pathways that connect the ADEP binding sites to N-terminal loops are rewired in this transition, with shorter network paths in the open pore configuration supporting stronger intra- and inter pling. Structural perturbations, either through the removal of ADEP molecules or point mutations, alter the allosteric network to w coupling.

Published under an exclusive license by AIP Publishing. https://doi.org/10.1063/5.0139184

I. INTRODUCTION

tial in all kingdomsof life.^{1,2} BacterialCaseinolyticproteases (Clp) assistthese mechanismsy performing intracellulaprotein quality controller regulatory protein degradatselfcompartmentalized Clp nanomachines comprise a cenaturaellike peptidasesuch as ClpPand one or two ring-shaped ATPase to ClpP triggers gate opening to unleash the powed legiradathe two opposite ends of the peptidase. Complex formation,

which is dependent on ATP bindintightly regulates the degradation process to prevent uncontrolled protein destruction. Maintaining protein homeostasis at the cellular level is essenlated ClpP is catalytically inactive as access to its proteolytic chamber is precluded by axigates locked in a closed configuration, which allow diffusion of short peptides but hinder the entry of longer unfolded polypeptide chains and block internalization of folded proteins. Docking of one or two ATPase partners components such as ClpA or ClpX, which are axially stacked at tion mechanism. Upon recognizing SPs targeted for degradation through short peptide tags attached covalently at the of

polypeptide terminal the ATPase applies epetitive mechanical degradation activity?-31 Weaker complexes with only five IGL/F forces to effect SP unfolding and translocation through its narhoups are functional, albeit degradation proceeds at a reduced rate. central channel and to propagate the unfolded polypeptide to WaecN-terminalloops are also involved in the complex formathe peptidase core. SP degradation takes place processively ation through interaction with the ATPase pore-2 lobopseyever, yields small peptide fragments of 7–8 amin acids. they form weaker contacts due to their greater conformational Highly conserved N-terminabps (amino acids 1–19) conflexibility, 20,32,33 Remarkably, pore opening may be affected without

trol access to the degradation chamber through the axiarles regions (residues 123–148) of each protomer (Fig. 1). In the "clitsent envilalaning-methylproline and alanine moieties of the the proteolytic chamber. Removalof the N-terminalloops in the isolated peptidase to indiscriminately destroy unfolded prosimilar in the ADEP-bound and ClpX-bound configurationits)

assistance from the ATPase through strongly cooperative binding of of the double-ring tetradecameric Clipp. Intermediate "head" seven acyldepsipeptide 1 (ADEP1) molecules to the peripheral Clpp. regions (residues 20–122 and 149–193) connect N-terminal loopteto (Fig. 1). 2.34 Kinetic studies indicate that DEP1 establishes the inter–ring equatorial interface formed by interlocked "hand the orable interactions with the ClpP hydrophobic groove through pore configurationN-terminalloops assemble into a mesh that aliphatic tall. This triggers a dramatic conformational transition to involves strong inter-loop contacts and that ludes passage to a quasi-symmetric configuration of N-terminal β -hairpins pointing outward from the proteolytic chamber that results in nearly dou-ClpP variants abolishes the gating mechanism and enables evening the pore diameter. Notably, the ClpP structure is very teins. Functional control of degradation through complex formthe complex formt with the ATPase is mediated by contacts formed with a ClpP riming and 0.6 Å in the pore region (defined by the seven N-terminal at hydrophobic grooves located at periphetres from the axial loops and adjacent helices up P pore opening induced by ADEP pore Although docking of the hexameric ClpA or ClpX ATPasesbinding yields powerfultibacterialction through uncontrolled to the heptameric ClpP rings involves a symmetry mismatch, destruction of acterial proteins that s pursued for therapeutic binding of six conserved ATPase loopsich contain the IGL or applications against pathogenic Staphylococcus aureus and Mycobac-IGF sequence motif in ClpA or ClpXespectivelyensures robust terium tuberculosis, 38-41 Structurablasticity of ClpP probed in

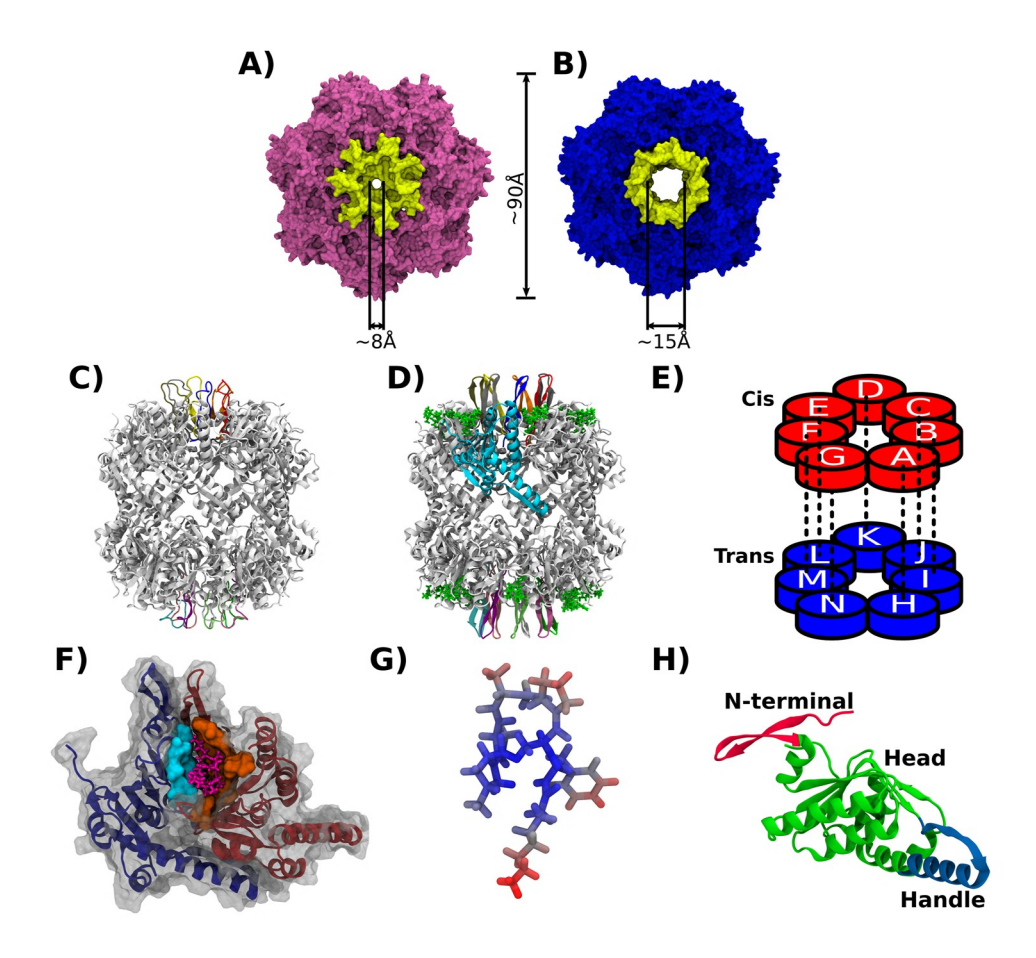


FIG. 1. Structural details of the closed and open pore configurations of ClpP. (a) and (b) The crystal structure of the (a) closed [Protein Data Bank (PDB) ID: 1YG6] and (b) open (PDB ID: 3MT6) pore configuration of ClpP [(a) pink; (b) blue] reveals dramatic gate-controlling conformational transitions of N-terminal loops (yellow) (c) and (d) Side view of the (c) closed and (d) open pore configurations of ClpP (gray). N-terminal loops (color-coded), ADEP1 molecules (green) and one ClpP protomer (cyan) are highlighted. (e) Protomer organization of the cis (red) and trans (blue) heptameric rings and cross-ring interprotomer coupling (dashes), mediated by the handle region interface, are indicated. (f) Top view of the ADEP binding site consisting of the hydrophobic pocket (indicated as a molecular surface) formed at the interface between chains A (blue) and B (orange). (g) ADEP1 molecular structure. (h) Domain architecture of ClpP monomer. N-terminal (residues 1-19, red), head (residues 20-122 and 149-193, green), handle (residues 123-148, blue) are highlighted. Molecular images in this work are rendered using Visual Molecular Dynamics.63

crystallographic and computatiostaldies led to the hypothesis 1000 kl/(mol nm). In the second equilibration step, the restrained that transient exit channels form in the equatorial region to facilistem was simulated for 500 ps in the NPT ensemble, with the contate the release of peptide fragments resulting from the degradatiopressure of 1 atusing the Parrinello-Rahmanlgorithm. The time step in allMD simulations was 2 fsFinally, restraints

The details of allosteric communications that underlie the wete removed andor each setutiour unbiased MD simulation ical gate opening mechanism remain elusive even as multiple diplectories (50 ns each) were performed in the NPT ensemble. For conformations have been resolved challenges are commonly analysis purposed frames were saved every 100 ps were saved noted for ring-shaped molecular machinesh as GroEL, therafter excluding the first 10 ns of each trajectory. Root-mean-square mosome and CCT chaperonias d are attributable to their largedeviations of simulations in each setup are shown in Fig. S1. conformational plasticity, namic rewiring of allosteric networks, and correlated intra- and inter-ring motions. To uncover the allosteric mechanisms in ClpRe use computational proaches that are able to address such questions in diverse proteins by probing between residue pairs the proteinwe computed the Dynamic the complex networks of sidue-residue interactions underlying cross Correlation Matrix (DCCM) of position fluctuations of C the long-distance communication between the effestite rand of strongly coupled amino acids and to map the allosteric pathways i and j: connecting them.

In this paper, we describe comparative studies of ClpP conformational dynamics in its open- and closed-pore configurations. To this end, we perform solvated, atomistic, molecular dynamics simulations of these systems and we identify the collective motions using principal component and normal mode analyses. Coupling between a function of time, (·) denotes the ensemble average over regions of the tetradecameric structure revealed by community let a function of time, (·) denotes the ensemble average over work analysis indicates a switch between inter- and intra-protomer denotes the instantaneous position fluctuation sides in the coupling as a result of the transition from the closed to the open for configuration. Allosteric paths identified between the ADEP binding its mean over the simulation time relation values range sites and the CIPP N-terminadops highlight stronger intra- and from -1 to 1, with positive & values corresponding to motions sites and the CIPP N-terminadops highlight stronger intra- and from -1 to 1, with positive & values corresponding to motions the open configuration.

II. METHODS

A. Molecular dynamics simulations

The closed and open pore configuration £sufherichia coli ClpP were described using the x-ray structures with Protein Data Simulation time per trajectory $t \le 50$ ns. Bank IDs 1YG69 and 3MT6,4 respectivelyUnresolved regions of the x-ray structures were modeled using the Modledoserver. To study the effect of perturbations on each structure, we considered protein regions address this limitations performed several point mutationshich were implemented using PyMOL (Table S1). For each configuration and sequence molecular dynamic $(\Box \mathcal{G}) = 0.6$) and the Girvan-Newman algorithmoleics (MD) simulations were performed using the Groma2022 package and the CHARMM36 all-atom force fielishe CGenFF molecule compatible with the CHARMM36 force field proby adding an appropriate number of Na ions for each setup (Table 1.In general for an ensemble D derived correlation netest descent algorithm for 50 000 steps with the convergence chtework?

rion of the maximum force value smaller than 1000 kJ/(mol nm). Next,the systems were equilibrated by performing NVT and NPT Principal component analysis dynamics. First, simulations were performed for 500 ps in the NVT Molecular Dynamics of omplex biomolecular systems proensemble using the V-rescated gorithm with T = 300 K, and by duce high-dimensional datasets comprising atomic positions saved restraining the heavy atoms of the protein with a spring constanted time ster glean information about the most significant

B. Dynamic cross correlation matrix (DCCM)

To quantify the time-dependentlirectional correlations atoms of protein residues using the Bio3D packageM is an the functionalite. These approaches use concepts in graph $N \times N$ matrix, with N equal to the number of residues, where each theory combined with residue-residue coupling derived from struc-turaldata or conformationalynamics to identify "communities" residues i and i:

$$C_{ij}(t) = \frac{\langle \triangle \mathbf{r}_i(t') \cdot \triangle \mathbf{r}_j(t') \rangle}{(\langle \| \triangle \mathbf{r}_i(t') /^2 \rangle (\| \triangle \mathbf{r}_j(t') /^2 \rangle)^{1/2}}.$$
 (1)

2023 inter-ring coupling between binding sites and N-terminal loops in the negative values indicate motions in opposite directions. Convertible open configuration gence of the DCCM matrixhown in FigS2, was assessed using $R(t) = (1/N_p) \sum_{(ij)} (C_{ij}(t) - C_{ij}(t-\tau))^2$, where A is the number of residue pairs and the time interval $\tau = 5$ M/se note that evaluation of R(t) using several τ values between 2.5 and 10 ns consistently yield $R(t) \le 0.001$. Here; is evaluated using data frames up to the

DCCM maps yield couplings between highly interconnected residue pairs that make it challenging to decipher correlated motion community detection using the strongly coupled residue pairs in mented in the cna()function in the Bio3D software package. In this approach the full residue network is split into highly server was used to generate force field parameters for the ADEP ra-connected communities but weakly inter-connected between communities In the Girvan-Newman algorithm he number of tein structure was solvated in a dodecahedral box with dimensions. ~122 × 100 × 100³ Awith water molecules represented using the Modularity quantifies how well a network is partitioned into com-CHARMM-modified TIP3P9 model. The system was neutralized munities. Since this is a probability measure, the values are between S1). The solvated system was energy minimized using the steep. It modularity above 0.7 indicates reasonable partitioning in a

conformational dynamics at a coarse-grained level one can employ this traversing through a given node used to identify the Principal Component Analysis. Here, we probe the functional important residues that contribute to the allosteric network. Analydynamics between the open and closed configurations of ClpPsixyof node degeneracy indicates that ~350 paths between the source performing PrincipaComponentAnalysis (PCA). In PCA, the and sink are sufficient for convergence. covariance matrix $(\langle \triangle \mathbf{r} \triangle \mathbf{r}_i \rangle)$ comprising positional uctuations

is diagonalized to determine the set of eigenvalues and eigenvectormal mode analysis and structural tors. PCA calculations are performed using the GROMACS analyzeixurbation method

tools q_covar and q_anaelqyhere q_covar generates both eigenvalues and eigenvectors by diagonalizing the covariance matrix and response of the modes to perturbation modeled the eigenvector rior to PCA calculationwe remove translation and number of amino acid residues in the structure he nodes are ing each frame ofhe MD simulation onto the crystatructure. open and closed configurations is performed by calculating the nergy function: Mean Square Inner Product (RMSIP), which computes the overlap

In order to calculate the normal modes of the proteins and ana g_{anaeig} filters the original trajectory and projects it along a given as elastic networks composed of N nodes where N is the rotation degrees of freedom of the entire molecule by superimposed at the locations of thetoms of the amino acid residues in Ing each frame othe MD simulation onto the crystatructure. The comparison between the essential subspaces corresponding to the comparison between the essential subspaces corresponding to the comparison between the essential subspaces corresponding to the corres

between two subsets of eigenvectors by using,

$$RMSIP_{M} = \left(\frac{1}{M} \sum_{i,j=1}^{M} (\boldsymbol{\eta}_{i}^{A} \cdot \boldsymbol{y}^{B})\right)^{1/2}.$$
 (2)

each configuration account for over 80% of the total variance. between the residues in the PDB structure.

D. Optimal and suboptimal path analysis

To understand the dynamic coupling between the ADEP binding site and the N-termindbop regions of the ClpP ring, we calculate the optimal and suboptimal athstraversing from each ADEP binding site to althe N-terminaloops in one heptameric ringWe use the cnapath() function implemented in the Bio3D package. 72,75 In the path analysise ach C₁ atom is considered a node and the connection between nodes is weighted by $w_{ii} = -\log(||_{ii} \mathbb{I}|)$. To remove weakly correlated regions and interactions between residues that are not in contact, the DCCM is filtered δy is the perturbed spring constant. The sum is over all other using the cutoffvalue $|_{ii}C| \ge 0.3$ and the dynamic contacts obtained in the MD trajectorieshe contact map is generated in dynamically significant a specific residue is to a given mwde. residue pairs with the \mathbb{C}_{α} distance $d \leq 10$ Å present in at least the average value for a mode as significant. 75% of the simulation time frames. Next, the dynamic contact \simeq 2% of new contacts. Paths are determined by using an efficient dissed configurations according to the formula, rectional approach that simultaneously initiates the search from one "source" (ADEP binding site) residue and one "sink" (N-terminal loop) residue and identifies closed paths upon locating common nodes. The path with the shortest length is identified as optimal,

where y is the spring constant that defines the energy is take, d Here, the overlap is computed such that the top M eigenvalues \mathbf{q}_{M} namic distance between residues i and \mathbf{q}_{i} is the distance

 $H = \frac{1}{2} \sum_{i.i:d_i^0 < R_c} y (d_{ij} - d_j^0)^2,$

The normalmode calculation yields a set of 3N-dimensional eigenvector and corresponding eigenvalues are each mode M. We also analyze the responses of these modes to perturbations that mimic to point mutations of specific amino acids. This approach has been termed the Structural Perturbation Method (SAM) in practice, we calculate the response to a mutation at the site i:

$$\delta\omega_{M} = \frac{1}{2} \sum_{i:d_{i} < R_{c}} \delta \gamma (d_{ij} - d_{j}^{0})^{2}, \tag{4}$$

nodes in the networkThe greater the response ω the more two steps. First, we identify persistent contacts in each trajectoright the nodes that have வெடி but are three-fold above

The overlap function quantifies how a given normal mode commap is generated as the consensus map of contacts identified in the conformation along a transition pathway. least three of the four trajectories. We find that the dynamic compacts mpute the overlap function by projecting the eigenvector q maps include $\simeq 84\%$ of contacts present in the native structure and iven mode M onto the displacement vector between the open

$$I_{M}^{open \to closed} = \frac{\sum_{i=1}^{N_{p}} \boldsymbol{q}_{iM} \Delta \boldsymbol{r}_{i}^{open \to closed}|}{\left[\sum_{i=1}^{N_{p}} \boldsymbol{q}_{iM}^{2} \sum_{i=1}^{N_{p}} (\Delta \boldsymbol{r}_{i}^{open \to closed^{2}})\right]^{1/2}},$$
 (5)

whereas slightly longer paths that are closed are identified as suboptimal. Accordingly, analysis of paths traversing between the "source" and the "sink" is useful to glean information about the allosteric regulation of regions that do not show large conformational changes. $p_i^{pen(closed)}$ are position vectors of the ith node in the open our analysis, 300 paths are calculated for each "source" and ith our analysis, 300 paths are calculated for each "source" and ith our analysis, 300 paths are calculated for each "source" and ith our analysis, 300 paths are calculated for each "source" and ith our analysis, and ith our analysis are position vectors of the ith node in the open ith our analysis ith ith our analysis ith it residue pair and path length distributions are analyzed to assessored) structures, respectively. A value of one for the overlap corstrength of the correlated motions. The extent of the overlap between to the direction given by the eigenweet and described the correlated motions. two path length distributions, i = 1, 2, is quantified by using with that of Δr . The relative amplitude of ode i in mode M is the overlapping coefficiency $\{a_i, b_j\}$ where $\{a_i, b_j\}$ thermore, the normalized node degeneracy, evaluated as the faraction components of the normalized eigenvector a_i

(3)

Closed

A)

Open

III. RESULTS

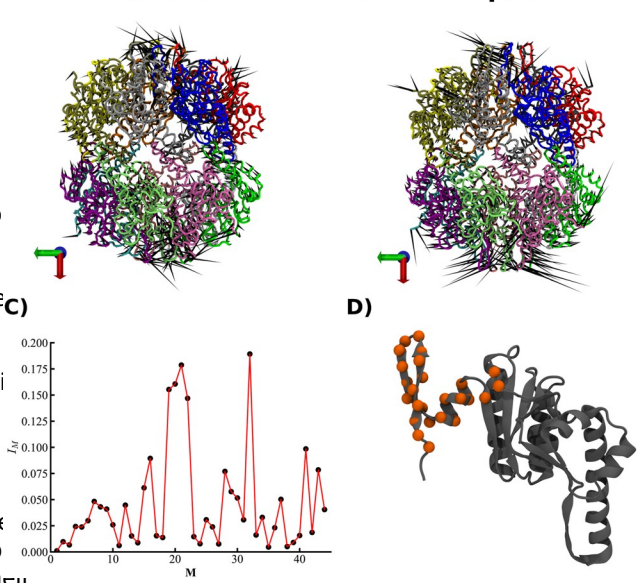
A. Collective motions underlying the gate-opening conformational transition involve primarily N-terminal loop regions of ClpP

To glean the collective motions of IpP protomers underlying the gate-opening transitione use NormaMode Analysis (NMA) and PrincipalComponentAnalysis (PCA) (see Sec.II). These approaches have proved highly effective in studies of co mational changes and dynamics of multisubunit biomolecules, as the ring-shaped chaperonins, ClpXP, or immunoglobulin. We use these analysis methods in conjunction to obtain detaile information abouthe collective motions as inter-residue couplings in NMA are restricted to an elastic network monthle native protein structure, whereas in PCA they reflect dynamic, i native as wells non-native contacts Nonlinear contributions to these couplingsquantified by considering the mutuial formation between residue coordinates ave also been used to probe allosteric networks. 60,61,94-9 We note that a recent study of the tetracycline repressor dimer identified similar trends in the inte 0.02 residue coupling when comparing linear and nonlinear contrib tions. A distinct advantage of network-based approaches is them ability to probe the propagation of allosteric signalmescales accessible to MD simulations, yet yielding results consistent w much longer biological timescales.

In PCA, diagonalization of the covariance matrix of tomic fluctuations yields the set of independent modes of motions of protein that characterizes its essentible space. Eigenvectors of the matrix characterize the orthogonal directions of maximal value ance, whereas eigenvalues determine the amplitudes if ional deviations. We focus on the PC modes that correspond to the largest eigenvalues (Fig. S3), which provide the major contribution subunits of each ring to enable the transition also note that

to the variance of fluctuatio its. the open state of Clo ive find that eigenvalues corresponding to the top 3 PC modes contribtite lowest frequency modebich describe global motions of the ≃40% of the cumulative variance of the fluctuation and eigen-ClpP tetradecamerave small contributions to the open \rightarrow closed values of the top 20 modes are required to explain $\simeq 67\%$ nef pore transition, whereas the five higher frequency modesich total variancen the closed statthe top 3 eigenvalues contributedescribe more local motions, are more suitable to describe the tran- \simeq 52% of the total variance whereas the top 20 eigenvalues consistently, the amplitudes of residue motions in the top tribute ≈74% of the total variance. In both cases, examination fix fether odes indicate large values only in the loop regions and negligi N-terminaloops that enable pore opening and closing Hals. ing motions More specifically the open state C1 corresponds and head regions than in the N-terminal loop regions. PC2 corresponds to torsional motions of N-terminal lbothse

motions we perform normabde analysis of the open state con the average value able S2 shows the hot-spotesidues derived figuration (see Sea.). We focus on the subset of normalodes whose eigenvectors have the largest overlap (see) Swith the



B)

FIG. 2. Principal Component and Normal Mode Analysis for CIpP conformations (a) and (b) Motions corresponding to the first principal component (a) closed and (b) open pore configurations (see Movies SM1-6 in the supplementary material). (c) Overlap of normal modes of ClpP with amino acid displacements in the open → close transition. (d) The hot-spot residues (orange) extracted from the structural perturbation results. The list of hot-spot residues for the top two modes is shown

motions corresponding to the top 2 PC modes indicates a comble amplitudes outside of these regions (Fig. S4). These results revea nation of large amplitude swing-type and torsional motions of that dominant conformational changes in this transition are primarily associated with motions of the N-termloabs. On the basis and 2(b) and Movies SM1-4 in the supplementary material]. Hamfalle comparison between PCA and NMA results, we surmise that domains in the inter-ring interface undergo slight contracting twistmic fluctuations provide a stronger contribution in the handle to swing-like motions that underlie pore opening and closing and Hot-spot residues that are critical for allosteric communication are identified by employing the Structural Perturbation Method (see closed configuration, PC1 corresponds to torsional motions an紀 D. Here, the perturbations imposed by point mutations capcorresponds to a combination of swing-like and torsional motitums the change in the local network energy and hot-spot residues To discern the contribution of farmonic vibrations to these correspond to nodes whose responsing () & ceeds by three-fold

from the two modes with the largest over Bapand 28 (Fig.S5 and Movies SM5-6)and Fig.2(d) illustrates the location of these conformational changes corresponding to the transition betweent-theory residues projected onto a single CIPP monomer. We note open and closed conformations shown in Fig2(c), five modes that NMA and SPM analysis identify hot-spot residues clustered prihave overlap 0.15 €£ 0.2, whereas all other modes have smallearily in the N-terminal loop region, in accord with the dominant contributions (I < 0.1). The absence of a single, dominant, modern curval flexibility of this region in the harmonic approximation. indicates the lack of strong coordination of motions of the several addition to the hot-spotresidue cluster within and near the

N-terminalloops, SPM analysis highlights two residues (His191, intra-subunit coupling within six subunits that involves strong coordination between the N-terminabp, handle, and head regions Arg192) in the C-terminal region.

Both PCA and NMA results are consistent with observation [siq. 3(a)]. By contrast the limited coupling is observed across the of structural studies, which highlighted that the peptidase core, equatorial interface between protomers of the cis (A–G) and trans ClpP(20–193), has virtually identication formations in the open (H–N) rings (according to the ClpP protomer organization shown in and closed configuration on this basis, it was proposed that Fig. 1), involving the handle regions of two protomer pairs (C-J and ADEP1 binding causes a significant conformation and in the D-K). Removal of ADEP from the open pore conformation results N-terminal loops and only small-amplitude motions of the equiator amatic changes in intra-protomer coupling, which nearly abolrial belt formed between two 🎢 🗖 gauantify these contributions is the correlation between the handle region and the loop and to the motions and to pinpoint the regions with the largest configured regions [Fig3(b)]. Furthermore, the inter-ring coupling is bution to the open \rightarrow closed transition, further probe the PCs enhanced through coordinated motions and le regions offive associated with the motions the N-terminaloops and ofthe protomer pairs. These changes yield coupling patterns similar to the peptidase core, ClpP(20–193), respectively, in closed and open dosed conformation which intra-protomer coupling is weaker figurations. To this end, we perform separate PCA of each of tlaesceinter-ring coupling between handle regions of protomer pairs is two ClpP regions in each of the two configurations and we detprevialent [Fig. 3(c)]. We note that these results are consistent with the Root Mean Square Inner Product (RMSIP) of the two subsets@fmportant role of the handle domain in tetradecamer formation eigenvectors, which provides a measure of the similarity of motionstacking of the two rings (cis and trans). described by the PC modes (see Sec. II).

Comparison of collective motions of N-terminal loops was computed by considering the eigenvectors corresponding to the Optimal and suboptimal path analysis reveal largest 1 eigenvalues which collectively account or 80% of the variancethus representing the essential spaceQuantitatively, the overlap between the ssential subspace corresponding o N-terminal regions indicates weak similarity, with RMSIP ≈ 0.37 rehomers and the proximity of ADEP binding sites to the contrastfor the peptidase cor@pP(20-193),where the top 110 N-terminal loops suggest that allosteric signals can be transmitted eigenvectors must be included to describe the essential subspaces under relatively short, intra-protomer, paths. The ring structure of find a strong overlap between the PC modes, with RMSIP pprox 0.720 pHisowever, also allows effective allosteric communication to take indicates that ADEP binding has only a weak effect on the dynamics between ADEP binding site of one protomer and N-termina of the peptidase core. loops of the other intra-ring protom ₱csprobe these allosteric

Overall,NMA and PCA data suggest that the conformationahechanisms in a quantitative manner, we use approaches that compared the conformationahechanisms in a quantitative manner, we use approaches that compared the conformationahechanisms in a quantitative manner, we use approaches that compared the conformationahechanisms in a quantitative manner, we use approaches that the conformationahechanisms in a quantitative manner, we use approaches that the conformationahechanisms in a quantitative manner, we use approaches that the conformationahechanisms in a quantitative manner, we use approaches that the conformationahechanisms in a quantitative manner, we use approaches that the conformationahechanisms in a quantitative manner, we use approaches that the conformationahechanisms in a quantitative manner, we use approaches that the conformationahechanisms in a quantitative manner. transition of ClpP protomers during the gate opening and closingeresidue-residue positional correlations and concepts in graph best described by an ensemble of modken togetheboth PC and normal mode data reveal that large conformation changes only ctone ADEP binding site termed "source," and the seven exert at the N-terminal loop regions while the core remains mainterminal loops within one ring, or "sink." In the correlation netintact. work, each node represents one protein residue and the connecting

B. Distinct coupling between ClpP regions in closed and open pore configurations

edges that connect these nodes. We emphasize that, given the con-To investigate the correlated motions of regions in the Clpstruction of an allosteric map in the correlation space elative tetradecamewe employ the community network analysisch importance of the allosteric paths depends on the strength of the uses the residue-residue coupling quantified by the directionaboupling between constituent residue pairs rather than their proxcross-correlation map (DCCM, see Sec. II). DCCM maps are highlyity in the physical paceIn this framework the shortest paths interconnected at the residue levelch makes it complicated to between residues of esource and the sink revettle strongest extract information for large systems. Therefore, we probe complete couplings within a protein needs in the minimal nity network clusters by converting the atomic cross-correlatioleangth, or "optimal," path was notound to be very sensitive to to a coarse-grained type community network using the Girvanchanges in the protein configuration, therefore, analysis of allosteric Newman clustering methodo investigate both intra- and inter-communication limited to thipath may yield misleading conprotomer coupling select the cutoff of the cross-correlation clusions about the signaling pathwalks teads comprehensive between residues i andlifcl such that the maximum modularityanalysis requires the additional luation of suboptimal" paths, (see Sec.II and Fig. S6) corresponds to a larger number of com-which have slightly longer lengths than the optimal path. munity clusters than the number of ClpP protomers each Using this framework, we computed 300 paths for each residue of the three ClpP configuration and that this requirement is pair formed by one source and one sink amino aoidhis end, satisfied by $||\cdot|| \le 0.6$, which yields $\approx 30 - 40$ community clusters in lect as source one ADEP binding site [4(a)], comprising ClpP configurations (Tables S3–S5). As shown in Fig. 3, the commendues Val44, Leu48, Phe49, Glu51, Ala52, Phe82 from protomer nity network analysis reveals distinct patterns of domain coupling1 and Arg22 Leu23, Val28, Phe30 Tyr60, Tyr62, Ile90 Met92, in ADEP-bound and unbound conformations of Clarkingly, Leu114, Leu189 from the adjacent protomer i, and as sink two repthe ADEP-bound open conformation is characterized by extensive residues, Thr10 and Gly13, located near the turn of each

stronger coupling between allosteric and active sites of ADEP bound ClpP

The absence of large-scale rigid-body domain motions of ClpP

theory (see SedI). To this end, we map the allosteric paths that

edges have associated lengths that reflect the cross-correlation valu (see Sec. II). The path length between nodes located in the source

and sink is then identified as the sum of the lengths of all individual

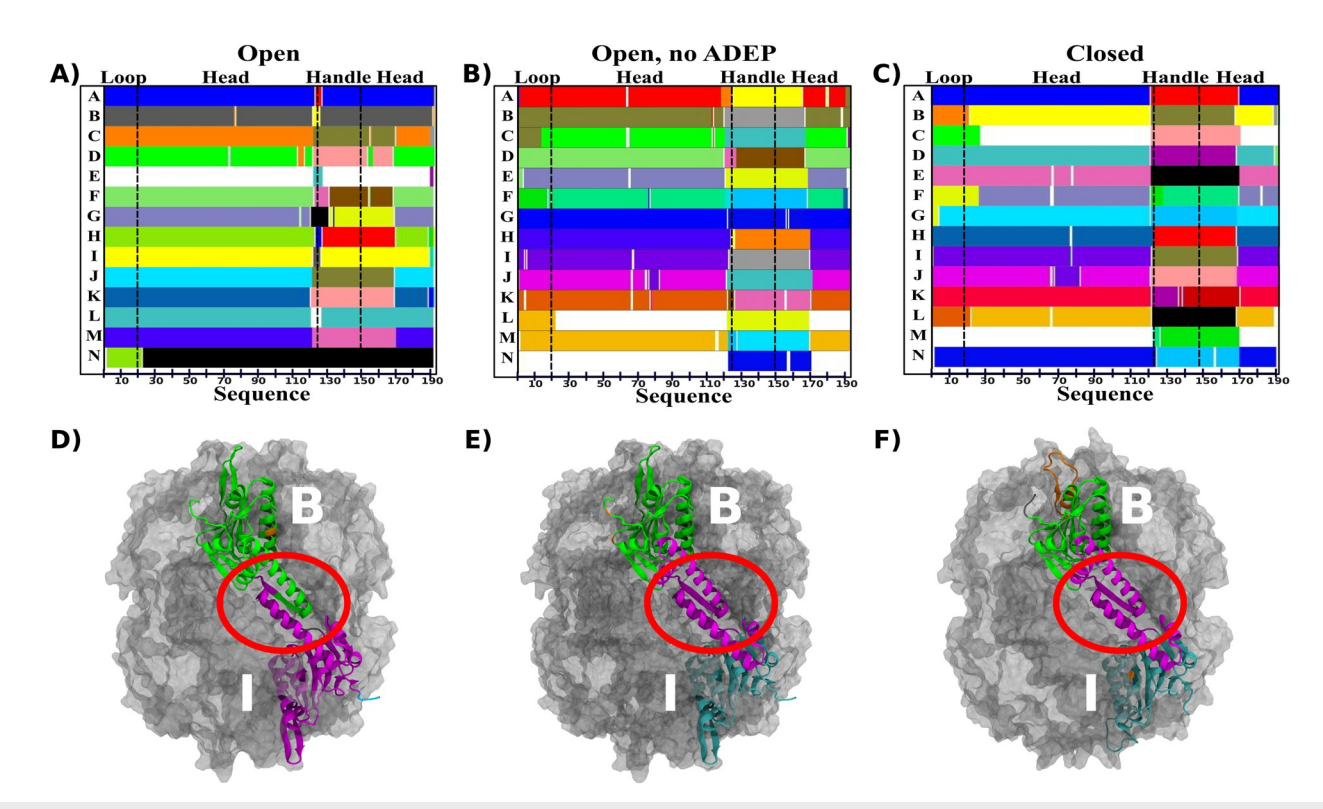


FIG. 3. Community network analysis for CIPP tetradecamer configurations. Community maps for (a) open pore (b) open, no ADEP bound (c) closed pore configurations. The N-terminal loop, head, and handle regions are indicated for the cis (protomers A-G) and trans (H-N) rings of ClpP. (d)-(f) Structural details of inter-protomer coupling across the CIPP rings. (d) Strong intra-protomer and weak inter-protomer coupling in the open pore configuration (e) and (f) Strong inter-protomer coupling mediated by the equatorial interface, including the handle region (highlighted by red elipse), in (e) open, no ADEP and (f) closed pore configuration. Communities identified in (a)-(c) are highlighted.

N-terminaloop in the same (cis) ring he selection of represendistribution toward paths of termediate lengths between those tative loop residues suffices for the purposes of mapping path found in the open and closed configuratives, we probed the the allosteric signal propagates within the loop exclusively thronoung a ring propagation of the allosteric signal by examining the path intra-loop residue by considering paths connecting each ADEP length distributions corresponding to paths connecting each bindbinding site to each loop, we examined a total of 470 400 pathwaysite to the N-terminadop of each protomer [Fig/sc)-4(f)]. traversing one ClpP ring (see Sed). In all three ClpP config-In accord with the above observations, path lengths corresponding urations the optimabathways are intra-protomeric and connecto the open state are consistently shorter than those for the closed Arg22 to loop residues 13–17 (Table 56) us, optimal pathways state. In both open and closed pore configurations, the shortest patl are largely stable among the three ClpP configuration, is in originating from the ADEP binding site of protomer *i* correspond to

paths in each pore configuration as wæslthe subsets of aths connecting each ADEP binding site to a specific loop [4(a)]. As shown in Fig.4(b), the histograms of suboptimath lengths in the three ClpP configurations highlighte stronger coupling shortest paths corresponding to the open By attentrastin the between the ADEP binding site and the N-terminal leepturbation of the open configuration through the removal of the ADME decay of the weaker allosteric signal in this Istatue dition, molecules results in a slighshift of the suboptimabath length

accord with observations made on small proteins noted abovepaths to the N-terminal loop of the same protomer [Figs. 4(c)-4(f)]. In order to characterize the strength of allosteric communitor open state, we find relatively short paths, of length \approx 2, to the tion from a broad perspective examine the set of suboptimal nearest neighbor loops in both clockwise (CW) and counterclockwise (CCW) directions. This strong intra-ring coupling supports the ability of the hexameric ATPase to trigger ClpP gate-opening even with the substoichiometric occupation of distal binding sites. Decreasing coupling strength is found in the N-terminal loops of the between binding sites and loops affected by ADEP binding, witsettoend and third nearest neighbor protomers, however, with slightly shorter paths in the CW direction [Figs. S7(A)–S7(C)]. In the closed closed statethe path length distribution is shifted toward longestate, we note the larger overlap than in the open state between paths with lengths up to \simeq 8 which indicates a weaker coupling path length distributions corresponding to neighboring loops and that of the same protomer loop which indicates a slower intrathe CW and CCW distributions corresponding to N-terminal loops

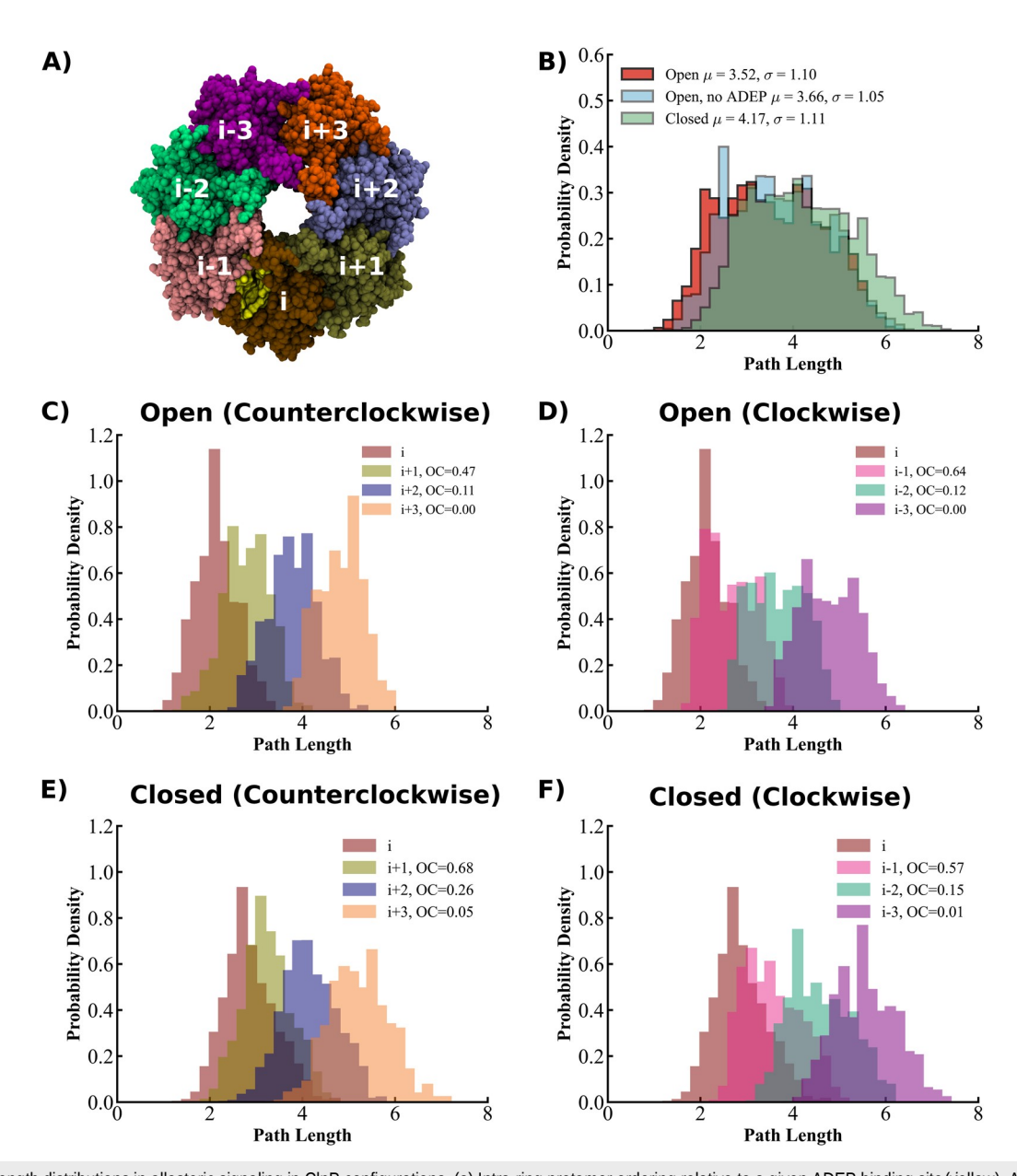


FIG. 4. Path length distributions in allosteric signaling in ClpP configurations. (a) Intra-ring protomer ordering relative to a given ADEP binding site (yellow). Allosteric paths are mapped between the binding site and the N-terminal loops in the same protomer i, and in protomers in counterclockwise (i + j, j = 1, 3) and in clockwise (i - j, j = 1, 3) directions. (b) Probability density distributions of path lengths are shown for the complete set of paths between each binding site and all intra-ring loops in the open (red); open, no ADEP (blue); and closed (green) configurations of ClpP. The legend indicates the mean and standard deviations of distributions. (c) and (d) Path length distributions of paths mapped in the open ClpP configuration between binding site i and loops in protomers in (c) counterclockwise and (d) clockwise directions are compared with the path length distribution of paths to the loop in protomer i. (e) and (f) Same as in (c) and (d) for the closed ClpP configuration. The legends indicate the overlapping coefficient, OC, between each distribution and the same protomer distribution.

of equidistantiearestneighbors overlap nearly completely [Figs.communicationTo obtain the microscopic understanding the S7(D)–S7(F)]. changes induced by perturbations probe the detailed paths in

The distinct pattern of path lengths in the open and closed aon configuration. To this end, we examine the three-dimensional figurations of ClpP, as well as the marked effect of perturbation associated with suboptimal paths (Fig. 5). The structural maps the path lengths indicate a significant dynamic rewiring of allow feelings the open configuration indicate strong

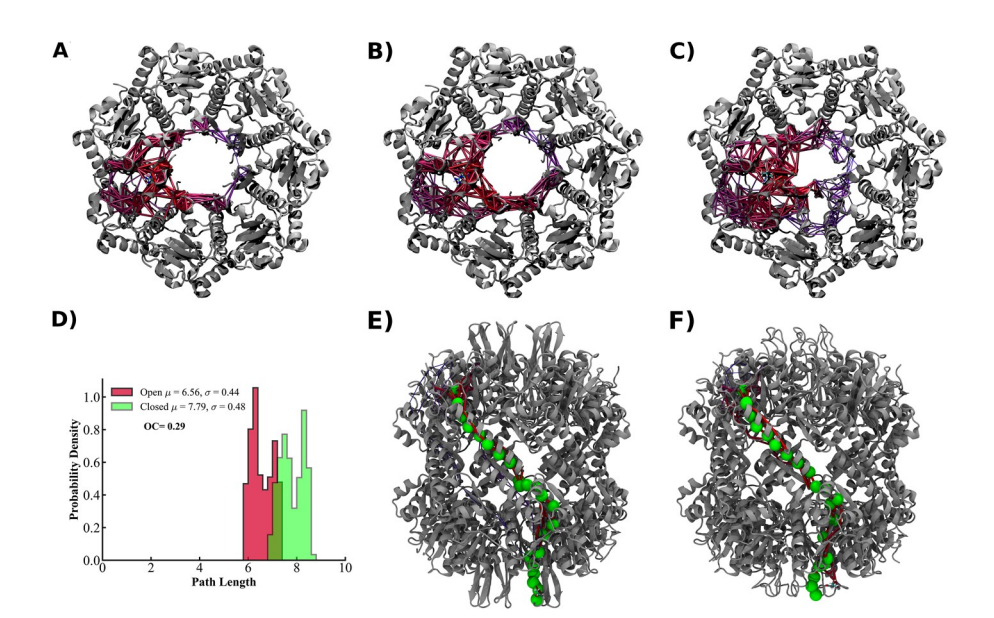


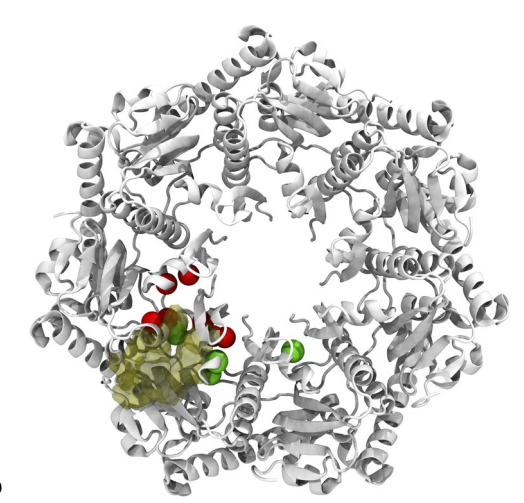
FIG. 5. Signaling pathways for ClpP configurations derived from the dynamic network analysis. (a)-(c) Suboptimal paths (red) between one ADEP binding site and all N-terminal loops in the same ClpP ring (gray) in (a) open; (b) open, no ADEP; and (c) closed pore configurations. (d) Probability density distributions of suboptimal inter-ring paths in open (red) and closed (green) pore configurations that connect the ADEP binding site of a cis ring protomer and the N-terminal loop in its *trans* ring protomer partner. The mean and standard deviations of distributions and the overlapping coefficient between them are indicated. (e) and (f) Structural details of the optimal inter-ring paths in (e) open and (f) closed pore configurations.

TABLE I. Normalized node degeneracy derived from suboptimal path analysis. Residues are grouped according to the ClpP protomer they belong to (shown as a subscript). Protomers are numbered in the counterclockwise direction, in the top view of the *cis* ring. In the path analysis, the ADEP binding site "source" includes residues from protomers i and i-1. Highlighted residues represent critical nodes (degeneracy ≥0.10) in all three ClpP configurations examined.

Residue	Ser21 ₋₁	Leu24 ₋₁	A	Ala45 _{−1}	Gln46 ₋₁	Leu5Q ₋₁
Open	0.17	0.26		0.07	0.14	0.19
Open, no ADEP	0.17	0.26		0.08	0.14	0.15
Closed	0.14	0.17		0.11	0.14	0.17
Residue	Ile19	Tyr20	Ser21	Leu24	Ile29	Ser21 ₊₁
Open	0.22	0.11	0.19	0.11	0.10	0.06
Open, no ADEP	0.11	0.19	0.26	0.12	0.08	0.13
Closed	0.16	0.23	0.22	0.05	0.09	0.06

signaling propagated from the ADEP binding site to the nearest three N-termindbops in the *cis* ring [Fig5(a)]. Removalof the ADEP molecules yields weaker coupling (indicated by thinner lines connecting the nodes) and increasing numberaths connecting the ADEP binding site to the more distant loops [Figb)]. In the closed configuration that connect multiple loops are increasingly found [Fig. 5(c)].

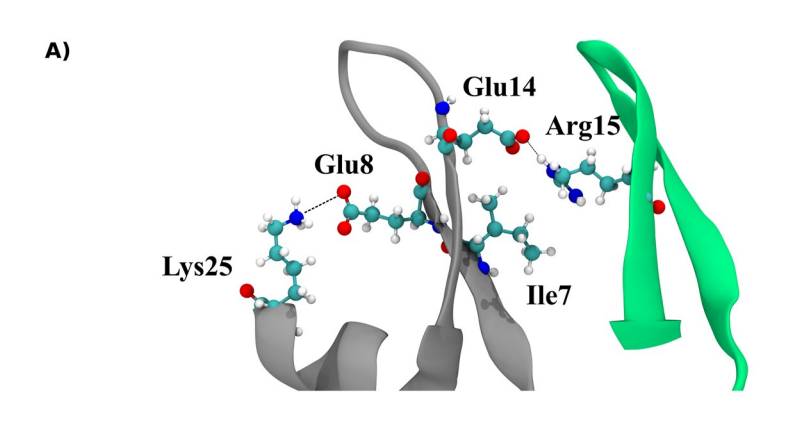
Interestingly shown in Fig5(d), the analysis of inter-ring pathways connecting the binding site of one protomer (B) in the *cis* ring and the N-terminabops of its partner (I) in the *trans* ring, using $|_{ij} O| \ge 0$ Reveals shorter paths of therefore ighter interring coupling, in the open configuration compared with the closed configuration. In the open configuration, allosteric communication between rings is primarily mediated by paths with lengths ≤ 6.5 , which are not available in the closed configuration, and the overlap between the two distributions is small, the overlapping coefficient $OC \simeq 0.29$ [Fig6(d)]. Although as noted in SedII B, the

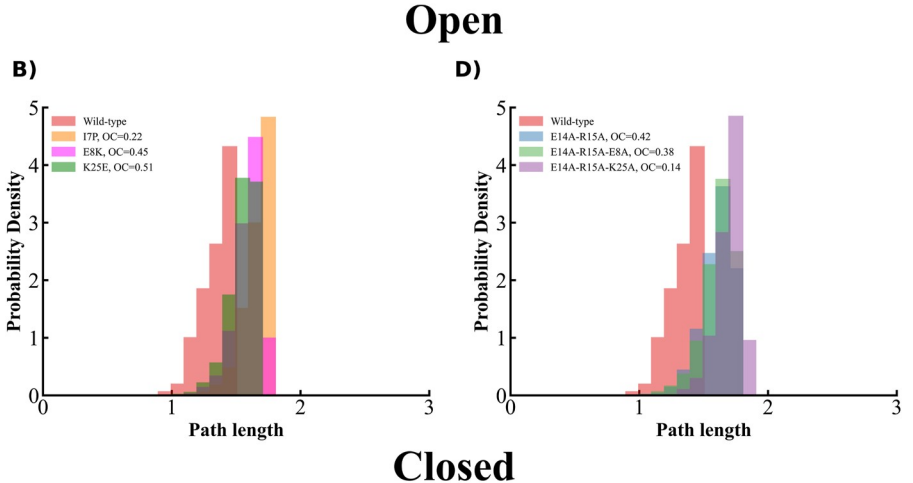


ficient $OC \simeq 0.29$ [Fig.(d)]. Although as noted in SedII B, the inter-ring handle interface is abolished in the open configurations are indicated with red (green) dots.

in Figs. 5(e) and 5(f). The shorter path lengths corresponding tinthe-protomegap must be crossed to connect the cis and trans open configuration can be rationalized in terms of the connectivity omer communities [Figs. 3, 5(e), and 5(f)]. The differential gap mediate the inter-ring allosteric communication, indicated in Fconfiguration and ≃6.9 for the closed pore configuration, as Whereasin the closed configurationaths mustross two gaps between intra-protomer communities to connett the interprotomer handle community, the open configuration, single,

between community networks of the cis and trans protomers the talty results in a length of \approx 5.9 for the optimal path in the open the structural details of the paths are similar (Table S7). We surmise that the handle interface, rather than facilitating inter-ring allosteric communicationacts as a constrainin the closed configuration,





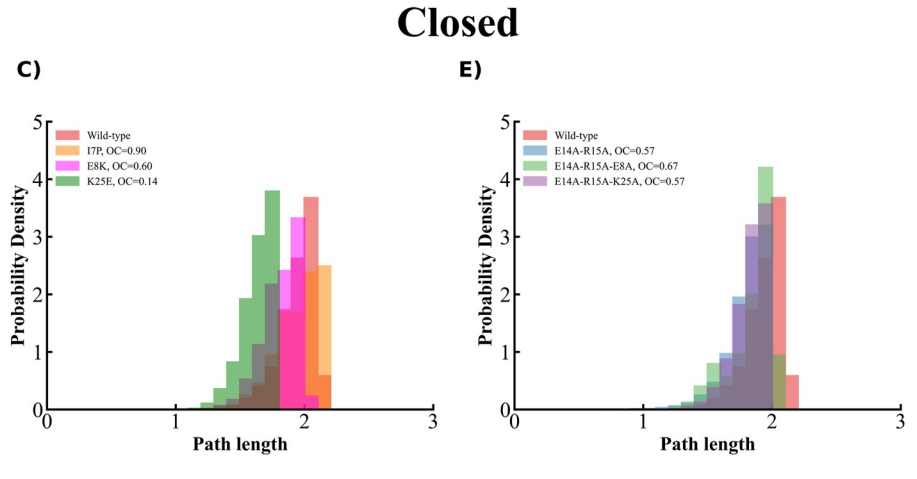


FIG. 7. Effect of mutations on allosteric signaling. (a) Single point-mutations considered, I7P, E8K, and K25E, affect the stability of individual loops (gray) and double and triple mutations, E14A-R15A, E14A-R15A-E8A, and E14A-R15A-K25A, affect both intra-loop and inter-loop (gray and green) stabilization. Salt bridges formed in the open pore configuration are highlighted. (b) and (c) Comparative probability distribution of the shortest 5000 paths in wild-type and single mutants in (b) open and (c) closed pore configurations. (d) and (e) The same as in (b) and (c) for double and triple mutants. Overlapping coefficients between each mutant and the wild-type distribution are indicated in the legend.

resulting in two intra-protomer path length penBltiesntrast, and a single path length penalty is applied.

ing, we compute the normalized intra-ring node degeneracy, closed state even in the wild-type ClpP [Figs. 7(d) and 7(e)]. We find the fraction of paths that include each node (see Lable I lighted in (Fig. 6). Notably, residues [JeTl/920, Ser2], Ser2], Ser2], and Leu241, at the base of N-terminal loops proximal to the ADEP binding site and Gln46 and Leu501, which are in the proximity of ADEP binding site, have node degeneracy ≥0.10 in all three setups and therefore are likely to have a critical tribution to allosteric communication. (In our notation, residue labelia@-opening conformationalnsitionIntriguinglythis transi-"source" binding site occupying protomers i-1 and i. Protometherelling N-terminal pop region. How is the allosteric signal ring.) One set of residu**e**ke19, Ser2 L_1 , Leu2 L_1 , and Leu5 L_1 , has a slightly reduced degeneracy in the closed pore configuration of the open and closed pore configurations of ClpP by performing and upon removalf ADEP molecules in the open configuration, equilibrium MD simulations afach ofthese states our results, whereas the other residues have increased degendateiesstsubstrate translocation in the ADEP bound open state.note that Ile19 is present in all three setups with a slightly higher value in a critical or the gate opening transition of p. We find the open setup.

D. N-terminal mutations differentially alter allosteric communication in open and closed pore configurations

We further explore how perturbation after the coupling mutations at N-terminaltes indicated to be functionally impor-eracy calculations indicating these residues as critically important (see SecI and Table S1).00 We focus,on the one handon single point-mutationsuch as I7PE8K, and K25E, that alter the stability of individual N-terminal loops, and, on the other handapencritical for the integrity of the N-terminal loops. double, E14A-R15A, and triple, E14A-R15A-E8A and E14A-R15A-(Fig. 7). To this end, we compare the path length distributions between each ADEP binding site and N-terminals of distant pathways connecting one binding site tothed ClpP N-terminal loops in the *cis* ring (see Sec.II). As shown in Fig. 7, we find that mutations have distineffects on allosteric couplinghich can manifest differently in the open and closed pore configura-is also strengthened in the open configurate men as the hanand closed configuration s shown in Fig. 7(b), the I7P mutation, which makes the coikonformation more favorables a drastic effect on the open configuration a low OC $\simeq 0.22$, accord with the deleterious effect of this mutation on polypeptideltiple communities in the closed configuration. degradation E8K and K25E mutations which remove the stabilizing salt bridge at the base of the N-termlored, affect both the open and closed configurations [π (\pm)], and τ (c)], which is consistent with their diminished degradation rates of both polyimep ClpA, and with the substrate protein being degraded to tides, which stringently require an open gantel, peptides which may be internalized through the closed gateouble and triple

mutations, including the E14A-R15A mutations that provide stabiin the open configuration, the inter-protomer constraint is remlizived inter-loop salt bridges, have a lesser effect on the closed than on the open pore configuration, as the salt bridges formed by Glu14 Next, to identify residues that are critical for allosteric signahd Arg15 residues in neighboring protomers are not present in the

that the triple mutation E14A-R15A-K25A has the strongest effect summarizes the residues in the cis ring that have the node degeneral losteric paths, with OC $\simeq 0.14$ in the open configuration, which $acy \ge 0.10$ in at least one configuration, as revealed by path anixing inaccord with the largest reduction in the degradation rate of The structural location of residues that act as critical nodes is **lpigly**peptides compared with the single and double mutations.

IV. DISCUSSION

Our computational tudies probe the allosteric mechanisms of the ClpP peptidase in response to effectothat activate its includes as subscript the protomer location in the cis ring, with the involves limited structural rearrangement outside of the gatenumbered in the counterclockwise direction in the top view of begagated in the absence of large-scale rigid-body motions of ClpP subunits? To address this question, we undertook comparative stud-

quantified through principalmponent and normalode analyingly, we also note that residue Gln46hows no change in node sis, highlight the similarity of motions of the peptidase core in the degeneracy values in the three seinutisating a weak sensitivity two states even as the loop motions are significantly different. to structural perturbations. Structural studies revealed that the presence analysis, both structural perturbation, derived from Norence of Ile19 is crucial for the stability of the N-terminal loops and Mode calculations, and node degeneracies, computed using the positional cross-correlationist hlighted a set of hot-spot residues

that the hot-spots derived from the harmonic approximation use in NMA reveal regions that are highly flexible and dynamic through their proximity to the N-terminal regions or the C-terminal regions. Node degeneracy values erived from dynamic rosscorrelations accounter hot-spotresidues that distributed in :3 both N-terminal loops and protease core. Here we note that residue between the allosteric and active sites of ClpP by engineering Deita, Tyr20, and Leu24 were common to both SPM and node degen-

> allosteric regulatio@ur results are in agreement with structural studies,00 which have shown that large non-polar side chains of Ile Our detailed analysis of intra- and inter-ring allosteric path-

K25A, mutations that affect intra-as well as inter-loop stabilizations reveals stronger communication in the open configuration responding to shortest 5000 suboptimal paths among the allosteriomers. According to these results, in this configuration, neighboring intra-ring protomers are strongly couplers istent with the observed ability of the ATPase to trigger gate opening even as it activates only six binding sittesterestinglynter-ring coupling tions. Single mutations have generally large effects in both opedle interface present in the closed configuration between protomer partners is removed. Stronger coupling in the open configuration is affected through efficient crossing of a single gap between residue communities that reduces the penalties of sing gaps between

Allosteric communication in the ClpP peptidase is likely to be further modulated by two externators pamely its interactions with the ATPase partner, such as the single-ring ClpX or the doubleeffect of the ATPase interaction reflects the variability of IGL/IGF loop binding to the seven ClpP binding sites during the catalytic

cycle. Given the asymmetric binding office six ATPase loops to and MCB-2136816 to G.S.This work used the Extreme Science the seven binding sites @IpP, it is plausible thathe signaling and Engineering Discovery Environment (XSED) ich is supinduced by ADEP binding represents the upper bound to the cpurted by NSF Grant N&CI-1548562XSEDE Bridges resources Additionally, the non-concerted conformation and itinates a street tion TG-MCB170020 to G. Partial support was received through ATPase hexamer further weakens the allosteric coupling and breesdearch cyberinfrastructure resources services provided by the ring symmetry Nevertheles symmetric intra-ring allostery the Advanced Research Computing center the University of may support ClpP's active internalization of the polypeptide chaincinnati. in the degradation process through non-concerted conformational changes ofhe pore loopsIn supportof the active actionstud-

pling strength between binding sites and the ClpP N-terminal letothere Pittsburgh Supercomputer Center were used through alloca-

ies using a ClpAP complex with one or more IGL loops of ClpA covalently crosslinked to the ClpP binding sites allow degradat@nflict of Interest

to proceed at a slightly reduced rate compared with the noncovalent. The authors have no conflicts to disclose.

ClpAP complex⁰¹

Allosteric communication within the ATPase itself has a high

Will are a page in Author Contributions complexity and carthereforegive rise to multiple responses in ClpP, but can be engineered to form a complex Withuitcomconfigurations f ClpB revealed distinctntra-ring communication within the nucleotide-binding domain (NBD) 1 and 29 ingssis (equal) Investigation (equal) ethodology (equal) alidation Whereas, in the NBD1 ring, strong coupling is found between (eggel); Visualization (equal). Hewafonsekage YasarF\u00f6nseka: and Small subdomains of neighboring subunits, in the NBD2 riconceptualization (equal) ata curation (equal) Formal analyintra-protomer coupling is dominant.

protein partneralso has the potentialto effect changes in the allosteric signaling noted in a recentstudy, ClpP forcefully grips the titin substrates with forces that exceed those of the pastalization (equal pi Wang: Conceptualization (equal pi wang: Conceptualizat ner ATPase^{1,03} Such strong signaling may dramatically alter thetigation (supporting) flethodology (equal) alidation (supportallosteric paths and break the symmetry of communications being subject to the the ADEP binding site and N-terminal loops.

SUPPLEMENTARY MATERIAL

mary of the MD setups for ClpP wild-type and mutantetups. Table S2 for hot-spot residues derived from the struptantalrnities and Tables S6 and S7 for the list optimal paths in each ClpP configurationFig. S1 for RMSD time series in each ClpP configuration, Fig. S2 for DCCM convergence computed over multiple trajectorie fig. S3 for the largest 20 eigenvalues b € PC modes for each ClpP configuratibiog. S4 for normalized amplitudes of amino-acid motions associated with the top five normal from the corresponding author upon reasonable request. of the ClpP tetradecame Fig. S6 for network modularity Fig. S7 for path length distributions f equidistant protomerloops, Movies SM1-4 for motions corresponding to principal components in the open (SM1–2) and closed pore configurations (SM3–4) and Wickner, M. R. Maurizi, and S. Gottesman, Science 286, 1888 (1999). Movies SM5-6 for motions associated with the top two normal modes.

ACKNOWLEDGMENTS

The authorsgratefully acknowledge stimulating discussions auer, eLife 9, e52774 (2020). with Sue Wickner and Mike Maurizi. This work has been supported atayama-Fujimur 6, Gottesmannd M.R. Maurizi, J. Biol. Chem. 262, by the National Science Foundation GranNos. MCB-1516918 4477 (1987).

ClpP. An illustration of the complex ATPase allostery is provide Ashan Dayananda: Conceptualization (equal); Data curation (lead); the double-ring ClpB disaggregase, which is not a cellular part Fermal analysis (lead); Investigation (equal); Methodology (equal); Validation (equal) Visualization (equal) Writing – original draft munity network analysis of apo, nucleotide and/or substrate-boxend; Writing – review & editing (lead). T. S. Hayden Dennison: Conceptualization (equal) ata curation (equal) Formal analysis (equal)Investigation (equal)Jethodology (equal)Jalidation The interaction between the ClpP peptidase and its substretqual); Visualization (equal Mohammad S. Avestarunceptualization (equal)Data curation (equal)Formalanalysis (equal); Investigation (equal) Methodology (equal); Validation (equal); (equal);Data curation (equal);ormalanalysis (equal);nvestigation (equal); Methodology (equal); roject administration (equal);

tion (equal), Writing - original draft (equal), Writing - review & See the supplementary material for Table S1 showing the soliting (equal). George Stan: Conceptualization (equal); Data curation (equal) Formal analysis (equal Funding acquisition (equal); Investigation (equal) ethodology (equal) roject administration bation method, Tables S3-S5 for highly correlated residue com(equal); Resources (equal) upervision (equal); alidation (equal); Visualization (equal) Writing - original draft (equal); Writing review & editing (equal).

Resources (equal) fixare (equal) alidation (equal) isualiza-

DATA AVAILABILITY

The data that support the findings of this study are available

REFERENCES

²M. Gersch, K. Famulla, M. Dahmen, C. Göbl, I. Malik, K. Richter, V. S. Korotkov,

P. Sass, H. Rübsamen-Schaeff, and T. Madl, Nat. Commun. 6, 6320 (2015). ³J. OrtegaH. S. Lee,M. R. Maurizi,and A. C. StevenJ. Struct.Biol. **146**,217 (2004).

⁴J. Wang, J. A. Hartling, and J. M. Flanagan, Cell **91**, 447 (1997).

⁵X. Fei, T. A. Bell, S. Jenni, B. M. Stinson, T. A. Baker, S. C. Harrison, and R. T.

```
<sup>7</sup>M. R. Maurizi, W. P. Clark, Y. Katayama, S. Rudikoff, J. Pumphrey, B. Bower<sup>f</sup>f, J. Zhang, F. Ye, L. Lan, H. Jiang, C. Luo, and C.-G. Yang, J. Biol. Chem. 286,
and S. Gottesman, J. Biol. Chem. 265, 12536 (1990).
                                                                                        37590 (2011).
<sup>8</sup>K. M. Woo, W. J. Chung, D. B. Ha, A. L. Goldbergand C.H. Chung, J. Biol.
                                                                                        <sup>43</sup>O. Keskin,I. Bahar,D. Flatow,D. G. Covell,and R.L. Jernigan,Biochemistry
Chem. 264, 2088 (1989).
                                                                                        41, 491 (2002).
                                                                                        <sup>44</sup>W. Zheng, B. R. Brooks, and D. Thirumalai, Biophys. J. 93, 2289 (2007).
<sup>9</sup>M. W. Thompson$. K. Singh,and M.R. Maurizi,J. Biol. Chem. 269, 18209
                                                                                        <sup>45</sup> M. Jayasinghe, P. Shrestha, X. Wu, R. Tehver, and G. Stan, Biophys. J. 103, 1285
<sup>10</sup>S. Gottesman, M. R. Maurizi, and S. Wickner, Cell 91, 435 (1997).
                                                                                        (2012).
11 K. R. Schmitz, D. W. Carney, J. K. Sello, and R. T. Sauer, Proc. Natl. Acad. Scf. R. Gruber and A. Horovitz, Chem. Rev. 116, 6588 (2016).
                                                                                        <sup>47</sup>R. Gruber, M. Levitt, and A. Horovitz, Proc. Natl. Acad. Sci. U. S. A. 114, 5189
U. S. A. 111, E4587 (2014).
<sup>12</sup>M. E. Lee, T. A. Baker, and R. T. Sauer, J. Mol. Biol. 399, 707 (2010).
                                                                                        (2017).
                                                                                        <sup>48</sup>A. R. Atilgan and C. Atilgan, Briefings Funct. Genomics 11, 479 (2012).
<sup>13</sup> M. W. Thompson and M. R. Maurizi, J. Biol. Chem. 269, 18201 (1994).
13 M. W. Thompson and M. R. Maurizi, J. Diol. Chem. 205, 1620, 179, 202 (2012). R. Nussinov, C.-J. Tsai, and B. Ma, Annu. Rev. Diophys. 22, 163 (2012). Struct. Biol. 179, 202 (2012). Solv. A. Feher, J. D. Durrant, A. T. Van Wart, and R. E. Amaro, Curr. Opin. Struct.
<sup>17</sup>A. Martin, T. A. Baker, and R. T. Sauer, Nat. Struct. Mol. Biol. 15, 1147 (2008). Guo and H.-X. Zhou, Chem. Rev. 116, 6503 (2016).
1/A. Martin, T. A. Baker, and K. T. Sauer, 1940, School, 18 C. Lee, M. P. Schwartz, S. Prakash, M. Iwakura, and A. Matouschek, Mol. School, 18 C. Lee, M. P. Schwartz, S. Prakash, M. Iwakura, and A. Matouschek, Mol. School, 18 C. Chennubhotla and I. Bahar, Mol. Syst. Biol. 2, e172 (2006).
19 M.-E. Aubin-Tam, A. O. Olivares, R. T. Sauer, T. A. Baker, and M. J. Lang, C54 A. Sethi, J. Eargle, A. A. Black, and Z. Luthey-Schulten, Proc. Natl. Acad. Sci. U.
                                                                                         6. A. 106, 6620 (2009).
145, 257 (2011).
<sup>20</sup> R. A. Maillard, G. Chistol, M. Sen, M. Righini, J. Tan, C. M. Kaiser, C. Hodges, I. Rivalta, M. M. Sultan, N. S. Lee, G. A. Manley, J. P. Loria, and V. S. Batista,
A. Martin, and C. Bustamante, Cell 145, 459 (2011).
                                                                                          roc. Natl. Acad. Sci. U. S. A. 109, E1428 (2012).
<sup>21</sup> A. Kravats, M. Jayasinghe, and G. Stan, Proc. Natl. Acad. Sci. U. S. A. 108, 224 Miao, S. E. Nichols, P. M. Gasper, V. T. Metzger, and J. A. McCammon, Proc.
                                                                                         Natl. Acad. Sci. U. S. A. 110, 10982 (2013).
(2011).
                                                                                        57 P. M. Gasper,B. FuglestadE. A. Komives,P. R. L. Markwick,and J. A.
<sup>22</sup>A. O. Olivares, A. R. Nager, O. Iosefson, R. T. Sauer, and T. A. Baker, Nat.
                                                                                        McCammon, Proc. Natl. Acad. Sci. U. S. A. 109, 21216 (2012).
Mol. Biol. 21, 871 (2014).
<sup>23</sup> A. Javidialesaadi, S. M. Flournoy, and G. Stan, J. Phys. Chem. B 123, 2623 (26) Scarabelli and B. J. Grant, Biophys. J. 107, 2204 (2014).
<sup>24</sup> A. Javidialesaadi, S. M. Flournoy, and G. Stan, J. Phys. A. T. Van Wart, J. Durr

<sup>24</sup> H. Y. Y. Fonseka, A. Javidi, L. F. L. Oliveira, C. Micheletti, and G. Stan, J. Phys. A. T. Van Wart, J. Durr

Comput. 10, 511 (2014).
                                                                                          A. T. Van Wart, J. Durrant, L. Votapka, and R. E. Amaro, J. Chem. Theory
Chem. B 125, 7335 (2021).
<sup>25</sup> R. A. Varikoti, H. Y. Y. Fonseka, M. S. Kelly, A. Javidi, M. Damre, S. Mullen, J. G. Palermo, C. G. Ricci, A. Fernando, R. Basak, M. Jinek, I. Rivalta, V. S. Batista,
Nugent, C. M. Gonzales, G. Stan, and R. I. Dima, Nanomaterials 12, 1849 (2017). A. McCammon, J. Am. Chem. Soc. 139, 16028 (2017).
                                                                                                                                                                                    August 2023
                                                                                          G. Stetz and G. M. Verkhivker, PLoS Comput. Biol. 13, e1005299 (2017).
<sup>26</sup>L. D. JenningsJ. Bohon,M. R. Chance, and S.Licht, Biochemistry 47,1031
                                                                                        <sup>62</sup>G. M. Verkhivker and L. Di Paola, J. Phys. Chem. B 125, 850 (2021).
                                                                                        <sup>63</sup> W. Humphrey, A. Dalke, and K. Schulten, J. Mol. Graph. 14, 33 (1996).
<sup>27</sup>S. G. Kang, M. R. Maurizi, M. Thompson, T. Mueser, and B. Ahvazi, J. Stru
                                                                                        <sup>64</sup>A. Fiser and A. Sali, Bioinformatics 19, 2500 (2003).
<sup>28</sup> A. Gribun, M. S. Kimber, R. Ching, R. Sprangers, K. M. Fiebig, and W. A. Hösinghrödinger, LLC, The PyMOL molecular graphics system, version 1.8, 2015.
J. Biol. Chem. 280, 16185 (2005).
                                                                                        <sup>66</sup> D. Van Der SpoelĘ. Lindahl,B. Hess,G. GroenhofA. E. Mark,and H.J. C.
<sup>29</sup> M. C. Bewley, V. Graziano, K. Griffin, and J. M. Flanagan, J. Struct. Biol. 15 3; erendsen, J. Comput. Chem. 26, 1701 (2005).
                                                                                        <sup>67</sup>R. B. Best, X. Zhu, J. Shim, P. E. M. Lopes, J. Mittal, M. Feig, and A. D. MacKerell,
113 (2006).
<sup>30</sup>Y.-I. Kim, I. Levchenko, K. Fraczkowska, R. V. Woodruff, R. T. Sauer, and TJra. J. Chem. Theory Comput. 8, 3257 (2012).
                                                                                        68 K. Vanommeslaeghe, Hatcher, C. Acharya, S. Kundu, S. Zhong, J. Shim,
Baker, Nat. Struct. Mol. Biol. 8, 230 (2001).
                                                                                        E. Darian,O. GuvenchP. Lopes I. Vorobyov et al.J. ComputChem.31, 671
<sup>31</sup> D. Y. Kim and K. K. Kim, J. Biol. Chem. 278, 50664 (2003).
                                                                                        (2010).
<sup>32</sup>Ž. Maglica, K. Kolygo, and E. Weber-Ban, Structure 17, 508 (2009).
<sup>32</sup> Z. Maglica, K. Kolygo, and E. Weber-ban, Screens T., T. Sauer, ACS Chem<sup>9</sup> E. Neria, S. Hischer, and IV. Karpius, J. English, J. Chem. Phys. 126, 014101 (2007).
<sup>34</sup>D. H. S. Li, Y. S. Chung, M. Gloyd, E. Joseph, R. Ghirlando, G. D. Wright, Y. O.M. Parrinello and A. Rahman, J. Appl. Phys. 52, 7182 (1981). Cheng, M. R. Maurizi, A. Guarné, and J. Ortega, Chem. Biol. 17, 959 (2010). <sup>72</sup>B. J. Grant, A. P. C. Rodriguesk. M. ElSawy, J. A. McCammonand L.S. D.
                                                                                        Caves, Bioinformatics 22, 2695 (2006).
<sup>35</sup>H. Brötz-Oesterhelt D. Beyer, H.-P. Kroll, R. Endermann, C. Ladel,
                                                                                        <sup>73</sup>H. Kamberaj and A. Van der Vaart, Biophys. J. 96, 1307 (2009).
W. Schroeder, Hinzen, S. Raddatz, H. Paulsen, Henninger, E. Bandow,
                                                                                        <sup>74</sup>M. Girvan and M. E. J. Newman, Proc. Natl. Acad. Sci. U. S. A. 99, 7821 (2002).
H.-G. Sahl, and H. Labischinski, Nat. Med. 11, 1082 (2005).
36 M. C. Bewley, V. Graziano, K. Griffin, and J. M. Flanagan, J. Struct. Biol. 16\vec{s}5 B. J. Grant, L. Skjærven, and X. Q. Yao, Protein Sci. 30, 20 (2021).
118 (2009).
                                                                                        <sup>76</sup>S. Hayward and B.. Groot, Molecular Modeling of Proteins (Spring 2008),
<sup>37</sup> S. Vahidi, Z. A. Ripstein, M. Bonomi, T. Yuwen, M. F. Mabanglo, J. B. Jurav 🙌, 89–106.
K. Rizzolo, A. Velyvis, W. A. Houry, M. Vendruscolo, J. L. Rubinstein, and L. E. A. Amadei, A. B. M. Linssen, and H. J. C. Berendsen, Proteins 17, 412 (1993).
                                                                                        <sup>78</sup> M. A. Balsera, W. Wriggers, Y. Oono, and K. Schulten, J. Phys. Chem. 100, 2567
Kay, Proc. Natl. Acad. Sci. U. S. A. 115, E6447 (2018).
<sup>38</sup>J. Kirstein, A. Hoffmann, H. Lilie, R. Schmidt, H. Rübsamen-Waigmann,
H. Brötz-Oesterhelt, A. Mogk, and K. Turgay, EMBO Mol. Med. 1, 37 (2009). A. Amadei, B. L. De Groot, M.-A. Ceruso, M. Paci, A. Di Nola, and H.J. C.
<sup>39</sup> P. Sass, M. Josten, K. Famulla, G. Schiffer, H.-G. Sahl, L. Hamoen, and H. BBëtzndsen, Proteins 35, 283 (1999).
                                                                                        <sup>80</sup> R. Cossio-Pérez, J. Palma, and G. Pierdominici-Sottile, J. Chem. Inf. Model. 57,
Oesterhelt, Proc. Natl. Acad. Sci. U. S. A. 108, 17474 (2011).
<sup>40</sup>R. M. Raju, A. L. Goldberg, and E. J. Rubin, Nat. Rev. Drug Discovery 11, 7326 (2017).
                                                                                        <sup>81</sup>X.-Q. Yao, R. U. Malik, N. W. Griggs, L. Skjærven, J. R. Traynor,
(2012).
<sup>41</sup>B. P. Conlon, E. S. NakayasuL. E. Fleck, M. D. LaFleur, V. M. Isabella,
                                                                                        S. Sivaramakrishnan, and B. J. Grant, J. Biol. Chem. 291, 4742 (2016).
K. Coleman, S. N. Leonard, R. D. Smith, J. N. Adkins, and K. Lewis, Nature 563L. E. Bradley, Overlapping coefficient," in Encyclopedia of Statistical Sciences
365 (2013).
                                                                                        (John Wiley, New York, 1985), Chap. 6, pp. 546-547.
```

- ⁸³ M. S. Weitzman,"Measures of overlap of income distributions of white anថិ O. F. Lange and H. Grubmüller, Proteins **62**, 1053 (2006). negro families in the United States," Technical Pap@2NdS Bureau of the Census, 1970).
- ⁸⁴ M. M. Tirion, Phys. Rev. Lett. **77**, 1905 (1996).
- ⁸⁵ I. Bahar and A. Rader, Curr. Opin. Struct. Biol. **15**, 586 (2005).
- 86 W. Zheng, B. R. Brooks, and D. Thirumalai, Proc. Natl. Acad. Sci. U. S. A. 1637. Yuan, J. Deng, and Q. Cui, J. Am. Chem. Soc. 144, 10870 (2022). 7664 (2006).
- ⁸⁷R. Tehver, J. Chen, and D. Thirumalai, J. Mol. Biol. **387**, 390 (2009).
- ⁸⁸O. Marques and Y.-H. Sanejouand, Proteins **23**, 557 (1995).
- ⁸⁹L. Skiaerven, A. Martinez, and N. Reuter, Proteins **79**, 232 (2011).
- ⁹⁰ M. Damre, A. Dayananda, R. A. Varikoti, G. Stan, and R. I. Dima, Biophys. **120**, 3437 (2021).
- 91 M. T. Posgai, S. Tonddast-Navaei, M. Jayasinghe, G. M. Ibrahim, G. Stan, $\frac{101}{100}$ 6. Kim, K. L. Zuromski, T. A. Bell, R. T. Sauer, and T. A. Baker, eLife **9**, e61451 A. B. Herr, Proc. Natl. Acad. Sci. U. S. A. 115, E8882 (2018).
- ⁹²L. González-PazÇ. LossadaM. L. Hurtado-LeónF. V. Fernández-Materán, J. L. Paz, S. Parvizi, R. E. Cardenas Castillo, F. Romero, and Y. J. Alvarado, AC(2003). Omega 8(8), 7302-7318 (2023).

- ⁹⁴L. G. Ahuja, S. S. Taylor, and A. P. Kornev, IUBMB Life **71**, 685 (2019).
- $^{95}\,\mathrm{M.}$ C. R. Melo, R. C. Bernardi, C. De La Fuente-Nunez, and Z. Luthey-Schulten, J. Chem. Phys. 153, 134104 (2020).
- ⁹⁶L. Astl, G. Stetz, and G. M. Verkhivker, J. Chem. Inf. Model. **60**, 3616 (2020).
- 98 M. Iljina, H. Mazal, A. Dayananda, Z. Zhang, G. Stan, I. Riven, and G. Haran, bioRxiv:2023.02.02.526786 (2023).
- ⁹⁹V. BhandariK. S. Wong,J. L. Zhou,M. F. MabangloR. A. Batey, and W.A. Houry, ACS Chem. Biol. 13, 1413 (2018).
- 100 J. AlexopoulosB. Ahsan,L. HomchaudhurN. Husain,Y.-Q. Cheng,and J. Ortega, Mol. Microbiol. 90, 167 (2013).
- ¹⁰² J. Weibezahn, C. Schlieker, B. Bukau, and A. Mogk, J. Biol. Chem. **278**, 32608
- ¹⁰³ S. D. Walker and A. O. Olivares, Biophys. J. **121**, 3907 (2022).